Analysis of Wrinkles and Corrugations in the Electrode Calendering Process

Zejun Fu[a,b], Zhutian Xu[a,b,*], Linfa Peng[a,b], Mingwang Fu[c,#]

[a] *State Key Laboratory of Mechanical System and Vibration, Shanghai Jiao Tong University, Shanghai, People's Republic of China*

[b] *Shanghai Key Laboratory of Digital Manufacture for Thin-Walled Structures, Shanghai Jiao Tong University, Shanghai, People's Republic of China*

[c] *Department of Mechanical Engineering, The Hong Kong Polytechnic University, Hong Kong, People's Republic of China*

Email address: fuzejun@sjtu.edu.cn, zjf2962@gmail.com (Z.J. Fu); zhutianxu@sjtu.edu.cn (Z.T. Xu); penglinfa@sjtu.edu.cn (L.F. Peng); ming.wang.fu@polyu.edu.hk (M.W. Fu)

Corresponding authors: Zhutian Xu; Mingwang Fu

[*] Zhutian Xu, Email: zhutianxu@sjtu.edu.cn.

[#] Mingwang Fu, Email: ming.wang.fu@polyu.edu.hk.

Analysis of Wrinkles and Corrugations in the Electrode Calendering Process

Abstract: Calendering is a crucial process in manufacturing of lithium-ion batteries electrodes. Wrinkles and corrugations of the electrodes are the main manufacturing defects in the calendering process, which present critical challenges in mass-production of lithium-ion batteries in industry. This study aims at studying the formation mechanism of wrinkles and corrugations during the calendering process. The corrugations in the coated area as well as the wrinkles in the uncoated area of the electrodes were revealed to be more dependent on the difference between the front and back tensions rather than the magnitude of the tensions. The tortuosity of corrugations was reduced by 34.2% at the tension difference of 20 N, compared to that of 5 N. Nevertheless, an increase in the tension difference led to an approximately linear increase of the shear displacement δ, causing severe wrinkles in the uncoated area of the electrodes. An analytical prediction model for the wrinkles during calendering was established based on the shearing of the rectangular membrane and an electrode quality evaluation method for balancing wrinkles and corrugations while maintaining a low-tension loading was developed. The optimal web tension conditions, at a tension difference of 17 N, was achieved to obtain the qualified calendered electrodes.

Keywords: batteries; calendering; wrinkles; corrugations; tension; modelling

Introduction

With high energy density, high power density and long cycle life, lithium-ion batteries have been employed in many fields such as electronic products, electric vehicles and grid energy storage. The increasing demand for high-performance and low-cost lithium-ion batteries results in challenges in the efficient electrode manufacturing process.[1-4] The manufacturing procedures for lithium-ion batteries consist of slurry mixing, coating, drying, calendering, slitting, vacuum drying and subsequent cell assembly and battery electrochemistry activation processes.[5, 6] Calendering is a crucial step in the electrode fabrication, which employs a high rolling load to compress the electrodes to a specified

thickness. Calendering not only increases the volumetric energy density, but also enhances the electrical and thermal conductivity, long-term cycle stability, and electrochemical properties of lithium-ion batteries.[7, 8]

The electrodes are typically composed of a metal foil, with aluminum for cathodes and copper for anodes, and a particulate composite material, with active ceramic powders for cathodes and graphite powders for anodes. The particulate composite is coated on both sides of the metal foil surface. Taking the cathode as an example, the thicknesses of the aluminum foil and single-side active coating are respectively 10-20 μm and 65-75 μm for commercial lithium-ion batteries.[9] In the calendering process shown in Figure 1, the electrodes are compacted to a required porosity by applying a line load of more than 1000 N/mm between two rolls with a diameter of up to 1000 mm.[10] A high compaction pressure and thickness reduction rate are required to realize high volumetric energy density, which results in significant elongations of the electrodes.[11] The elongation of the composite coating leads to evident corrugations in the coated area of the electrodes after calendering. In the existing process, web tensions are applied to the front and back ends of the electrodes to maintain the flatness during the calendering process. High web tensions are beneficial to reduce corrugations in the coated area, which at the same time lead to severe wrinkles in the uncoated area of the electrodes, as depicted in Figure 1. Corrugations and wrinkles adversely affect the subsequent slitting, stacking, welding, electrolyte filling processes and cell performance. In addition, the increase of tension leads to easier tearing of the ultra-thin foils. Frequent failures thus occur in the production lines with the rolling speed up to 100 m/min, which significantly reduces productivity and increases costs.

A few studies were conducted to examine the wrinkles and corrugations of electrodes during calendering process. Günther et al.[12] divided the calendering induced

defects into geometrical, structural and mechanical categories, and evaluated the impact of them on the subsequent cell manufacturing processes. They found that corrugations in the coated area affect electrolyte filling, gripping and handling processes, while wrinkles in the uncoated area impair contacting and welding. The corrugations and mechanical behavior of electrodes after calendering were investigated by Mayer et al.[13, 14] The compaction rate, types of coating materials, and uncoated current collector foil were revealed to affect corrugations, while the web tension was identified to have little effect. The same front and back tensions were involved in their research. Mayr et al.[15] developed a process control method for the calendering process via in-line data acquisition of electrode thickness and surface topography, leading to a promising reduction of waste and manufacturing costs. Abdollahifar et al.[16] revealed the formation of wrinkles was attributed to the different material deformation under the identical applied stress, which induced internal mechanical tension causing corrugations of electrodes. Schreiner et al.[17] investigated heat-assisted rolling during the calendering process. They found that the line load and mechanical stress throughout the process were reduced by heating. Therefore, the wrinkles of electrodes, especially at high line loads and high compaction rates can be reduced.

Numerical simulation models of the calendering process are also established as additions to the experimental analysis. Those works provide insights into the actual deformation of electrodes between two rolls. Zhang et al.[18, 19] conducted tensile and compression experiments to obtain the constitutive properties of porous electrodes. The mechanism of failure behavior of electrodes was identified by implementing the proposed constitutive models into finite element analysis. Gupta et al.[20] characterized the stress-strain relationship of active material layer in lithium-ion batteries by means of U-bending of one-side coated foils. A finite element model was established to validate

the properties of cathode active layer. In their model, an elastic-ideally plastic material was employed for the aluminum foil and an elastic material for the cathode active layer. An exponential model between the calendering line load and the coating density was developed by Meyer et al.[21, 22] The relationship between mass loading, active materials and compaction resistance was established. Zhu et al.[9, 23] obtained the mechanical properties of electrode coatings by compression tests in a specially designed aluminum mold. The deformation and failure sequence of lithium-ion battery components under mechanical loadings were simulated by employing the Drucker-Prager/Cap model in simulations. Sahraei et al.[24, 25] obtained the stress-volumetric strain curve from the uniaxial compression experiment of the cell and modeled the cell by finite element method using crushable foam model and predicted the load-displacement curve. Besides analytical and finite element models, calendering simulation by the discrete element method (DEM) provided a deeper understanding of electrode compaction.[26] However, the battery modeling scale involves six orders of magnitude, which limits the applicability of the DEM in electrode manufacturing process study.

According to the above reviews, wrinkles and corrugations of the electrodes during calendering process are critical problems in the manufacturing of lithium-ion batteries, which attract both industrial and academic attentions. However, a detailed understanding of those defects and process design methods are still lacking. In practical production, the mitigation of wrinkles and corrugations relies on experiences, resulting in high labor intensity, long commissioning time, waste of electrode materials and high scrap rates. To cope with those, this work aims to explore the mechanism of how the tensions during the calendering process affect the corrugation and wrinkles in the coated and uncoated areas, respectively. Calendering experiments of electrodes for lithium-ion batteries under different tension conditions were first carried out. A laser sensor-based

measurement and evaluation method of electrode wrinkles and corrugations was developed. The formation mechanism of electrode wrinkles and corrugations during calendering process and the effect of tension on them were explained by an analytical model for the wrinkles. Based on that, an optimal method to balance the corrugation and wrinkles of the calendered electrodes were established. The method presented is expected to shed light on the calendering process design and optimization for lithium-ion batteries.

Materials and methods

Electrodes

The uncalendered $LiNi_{0.5}Co_{0.2}Mn_{0.3}O_2$ (NCM523) cathodes were manufactured by MTI KJ GROUP, containing 95.5% active material, 2.5% carbon black and 2% binder, with a total thickness of about 160 μm. The active material was coated on both sides of a 16 μm thick aluminum foil at a surface mass loading of 29.3 mg/cm^2. The width of the coated active material was 200 mm and the width of the uncoated current collector foil was 40 mm. The geometry and appearance of the electrodes are presented in Figure 2(a) and (b).

Calendering apparatus

In the calendering process, the electrodes were continuously compacted with a two-roller calender MSK-2300A-E, as shown in Figure 2(a). The diameter and the width of calender rolls were 200 and 300 mm, respectively. The elastic deformation of the rolls was insignificant compared to the thickness difference between the active material and the foil.[27] Therefore, the rolls were considered as rigid bodies in the study. The coated electrodes were calendered at ambient temperature and a rolling speed of 2 m/min. The

applied line load was 1250 N/mm. The density of the electrodes increased from 2.03 to 2.87 g/cm^3 after calendering.

Based on the above apparatus, the following experiments were designed to explore the effect of the front and back tensions on the electrode wrinkles and corrugations. An experiment with no tension applied was first employed as a reference. After that, the detailed experiments design is summarized in Table 1. The front tension varied from 5 to 20 N with an interval of 5 N. Meanwhile, the difference between the front and back tensions was designed from 0 to 20 N with an interval of 5 N. In addition, two different uncoated foil width, i.e. 0 and 40 mm, were discussed to investigate its effect on the wrinkles and corrugations. The values of front and back tensions were adjusted by controlling the unwinder and rewinder presented in Figure 2(a). Three repeating tests were conducted for each experimental condition. After calendering, all the electrodes were cut into a square with a length of 100 mm to enable the measurement of electrode wrinkles and corrugations, as depicted in Figure 2 (b).

Measurement of electrode wrinkles and corrugations

To evaluate the magnitude of the wrinkles and corrugations, three-dimensional scanning of the calendered electrodes was performed using a Keyence LJ-X8020 laser profiler mounted on a three-axis motion stage. Figure 3(a) shows an overview of the measurement system. The accuracy of the laser sensor and motion stage were 0.3 μm and 0.1 μm, respectively. The laser sensor captured the height profiles of the electrodes along the x-direction (which is perpendicular to the running direction) at a frequency of 1000 Hz and the speed of the motion stage along the y-direction (which is in the running direction) was 10 mm/s. The three-dimensional topographies of the electrodes after calendering were obtained by stacking the obtained height profiles with an interval of 0.01 mm, as illustrated in Figure 3(b). Based on those, a measurement window with 8

mm along the width and 4 mm along the height for each specimen was constructed.

Results and discussion

Evaluation of wrinkles and corrugations

Wrinkles in the uncoated area and corrugations in the coated area are geometric defects that coexist on calendered electrodes. The quantification of wrinkles and corrugations were conducted for the sake of evaluating the degree of geometrical defects for calendered electrodes. As shown in Figure 4, based on the three-dimensional scanning results of the calendered electrodes, two height profiles at a distance of ±1mm from the junction of the coated and uncoated areas were extracted along the rolling direction, as illustrated by the dash lines l_1 for the coated area and l_2 for the uncoated area, respectively.

The wavelength of corrugations in the coated areas was revealed to fall in the centimeter range. The following data processing procedure was conducted to capture the major corrugation features after calendering: (1) smoothing: Savitzky-Golay filtering with a smoothing window of 300 data points was carried out to remove the minor fluctuations; (2) elimination of the overall electrode inclination after cutting: a straight line connecting the start and end points, which represents the overall inclination of the electrodes, was subtracted from the smoothed data. After those, the cross-section curve of corrugations in the coated area can be obtained, as shown in Figure 4 (a). In order to avoid excessive random errors caused by the direct use of the maximum height value of corrugations, the degree of tortuosity ΔC, was proposed as an evaluation index of the corrugations in the coated area. ΔC is the difference between the total length C of the coated area in the calendered electrodes and the length C_0 scanned by the laser sensor along the rolling direction, and the value of C_0 is 100mm.

In the uncoated area, short and dense wrinkles in the collector foil were the main geometrical defects. As illustrated in Figure 4 (b), the wavelength and amplitude of wrinkles were in the millimeter range. To capture the wrinkles characteristics in the uncoated area, the overall inclination of the electrodes and the centimeter-range corrugations of the coated area need to be eliminated from the raw data. To realize that, Savitzky-Golay filtering with a smoothing window of 100 data points was performed as a first step. After that a spline curve was fitted by the valley points of each wrinkle to represent the overall inclination of the electrode. Hence the values of the spline curve were subtracted from the data. Based on the processed cross-sectional curves of wrinkles, the ratio of amplitude to the half wavelength $R = A / \lambda$ was employed as the severity of wrinkles in the uncoated area.

Forming mechanisms of electrode wrinkles and corrugations

To investigate the cause of wrinkles and corrugations in the calendering process of electrodes, the results of experiments #1, #2, #8, and #11 were compared. The height profiles of the coated area and uncoated areas of the electrodes along the rolling direction under four different conditions, i.e. without uncoated current collector, no front and back tensions, equal front and back tensions, and greater back tension, were obtained.

As illustrated in Figure 5(a), in the absence of the uncoated collector, the coated area of electrodes was elongated after calendering and the electrode was not corrugated. In comparison with the case #2, where the uncoated collector was present, significant corrugations was observed in the coated area of electrodes. That is because the foil in the uncoated area is not in contact with the rolls and thus not elongated after calendering process. As a result, the foil hinders the elongation of the coated area, which results in out-of-plane bending and deformation of the coated area. Due to the elongation

mismatch between the coated and uncoated areas, corrugations in the coated area occurs. However, if the uncoated area was removed, the elongation of the coated area was not restricted, leading to the elimination of the corrugations, as shown in Figure 5(c).

In the presence of an uncoated collector foil, the front and back tensions had significant effect on the wrinkles and corrugations of the electrodes. As shown in Figure 5(a), when front and back tensions were not applied, evident out-of-plane corrugations could be observed in the coated area. Meanwhile, the millimeter-range wrinkles were not significant. By increasing both the front and back tensions to 10 N, similar corrugations and little wrinkles was observed in the coated and uncoated areas, respectively. Those observations are consistent with the results reported by Mayer et al.[28]

On the other hand, when keeping the front tension at 10 N while increasing the back tension to 25 N, the geometrical defect patterns of the electrodes changed significantly. The tortuosity of the corrugations in the coated area, which can be represented by the value of ΔC described above, was reduced from 0.36 to 0.27 mm, compared to the case that the front and back tensions were equal. Meanwhile, as shown in Figure 5(b) and (c), evident wrinkles in the uncoated area also appeared. Short and dense wrinkles appeared in the junction area near the uncoated side at an inclination angle of approximately 30 degrees to the direction of rolling.

In summary, increasing the front and back tensions simultaneously has little improvement effect on corrugations of calendered electrodes. On the other hand, the difference between the front and back tensions is the main parameter affecting the corrugations in the coated area and the wrinkles in the uncoated area. It should be noted that the deformation of the compacted active material occurred mainly in the thickness direction, with negligible deformation in the rolling and transverse directions.[13] Hence

the material flow along the rolling direction was small enough to ignore the velocity difference in the deformation zone as well as the shift of the neutral point. As shown in Figure 6, the coated area of the electrode is elongated in the rolling direction after calendering, and the back tension acts on the uncoated area that is not elongated, resulting in the current collector foil being stretched backward. Therefore, the difference in displacement between the two areas decreased and the hindering effect of the uncoated area on the elongation of the coated area is alleviated, thereby the flatness of the coated area is improved. At the same time, the uncoated area is stretched backwards to form evident wrinkles at the coating edge. In the cases where no tension is applied, the front and back tensions increase simultaneously or the front tension is greater than the back tension, there is no backward stretching effect on the uncoated collector, leading to little improvement of the corrugations on the electrodes.

Effect of web tensions on wrinkles and corrugations

To elaborate the effect of tension on the wrinkles and corrugations of the electrodes, the evaluation index ΔC for the coated area and the ratio R for the uncoated area, were obtained for all experiments. As shown in Figure 7(a), the tension difference remained 0 N while the front tension was 5 N, 10 N, 15 N, and 20 N, respectively. The results indicated that a simultaneous increase of the front and back tensions had little effect on ΔC. On the other hand, by controlling the front tension at a constant of 5 N, the tortuosity of corrugations decreased with the increase of the tension difference. As depicted in Figure 7(b), with the tension difference increased from 5 to 20 N, the value of ΔC decreased from 0.38 to 0.25 mm, for a reduction of 34.2%.

As illustrated in Figure 7(c), the height profiles of wrinkles in the uncoated area of the electrodes were obtained with different tension differences while making the front tension constant at 10 N. As the tension difference increased, the half wavelength of the

wrinkles decreased while the amplitude increased. That leads to the difficulty of elastic recovery of the wrinkles and permanent deformation of the current collector foil. As shown in Figure 7(d), the effect of the tension difference on the amplitude half wavelength ratio R of wrinkles was obtained. An increase in the difference between the front and back tensions led to a significant increase in the ratio R and more severe wrinkles in the uncoated area. That is due to the more evident misalignment between the coated and uncoated areas along the rolling direction induced by a greater tension difference.

To measure the difference in shear displacement, grid lines were scribed on the surface of the uncalendered electrodes using a scribing needle and the 3D topographies of the electrodes were recorded before and after calendering using a laser sensor described in the previous section. As shown in Figure 8, the difference in shear displacement δ between the coated and uncoated areas was obtained by comparing the deformation of the grid lines along the rolling direction before and after calendering. The shear displacement difference δ increased with the tension difference T_d, which could be described by a linear relationship:

$$\delta = 0.01 + 0.00508T_d \quad (1)$$

Analytical modelling of wrinkles

Based on the results obtained above, the difference between the front and back tensions is a major parameter affecting the wrinkles and corrugations of the electrodes. A balance of the wrinkles in the uncoated area and corrugations in the coated area under optimized web tension condition is the key for the calendering process control to minimize those geometrical defects. Thus, an analytical model for predicting wrinkles was developed to determine the optimal web tension conditions. The interaction between the coated area

and the uncoated area was attributed to the displacement difference and a prediction method for membrane shear wrinkling was employed.

The wrinkling is significantly affected by the geometric parameters, material properties and boundary conditions[29], to study the influence of web tensions on the wrinkling behavior, following simplified assumptions were made during modeling: Firstly, linear elasticity, small deformations and homogeneity of the material were assumed. Secondly, the collector foil underwent a uniform horizontal in-plane displacement along the coating edge. Finally, the wrinkles were assumed to be parallel and evenly spaced with the inclined angle of 35° to the rolling direction, according to the experimental observations of wrinkles after calendering. On the basis of the thin-plate bifurcation theory, as shown in Figure 9, the uncoated area of the electrode could be treated as a rectangular membrane with a width of H. The difference in displacement of coated and uncoated areas along the rolling direction was described by δ, and the shear angle γ, which could be calculated by $\gamma = \pi/180 \cdot \arctan(\delta/H)$.

Referring to the analytical model for predicting wrinkles in rectangular membrane proposed by Wang et al.[30], the collector foil deformed into a doubly curved shape, it is feasible to build a model that describes the wrinkled surface using the coordinate systems ξ and η. ξ is parallel to the wrinkle direction and η is perpendicular to the wrinkle direction, as shown in Figure 10. ξ and η were the major and minor principal stress directions of the membrane, respectively.

The length of the model is kH, $k = 1/\sin(35\pi/180)$ and the width is λ. The configuration of the out-of-plane displacement function was:

$$w = A \sin\frac{\pi\eta}{\lambda} \sin\frac{\pi\xi}{kH} \tag{2}$$

The stress in the ξ direction in the wrinkled region could be expressed as:

$$\sigma_{\xi} = E\gamma + \frac{\pi^2 Eh^2}{12\lambda^2(1-v^2)} \tag{3}$$

where E is the Young's modulus and has a value of 70 GPa, v is the Poisson's ratio and has a value of 0.33, and h refers to the thickness of the current collector foil.[24]

It was assumed that the critical wrinkling stress σ_{η}, perpendicular to the wrinkles, was equal to the stress necessary for buckling a simply-supported plate with an infinite length and a width of λ:

$$\sigma_{\eta} = -\frac{\pi^2 Eh^2}{12\lambda^2(1-v^2)} \tag{4}$$

The force equilibrium relationship along the out-of-plane direction of the membrane is given in Figure 10, and the equilibrium equation could be expressed as:

$$\sigma_{\xi} k_{\xi} + \sigma_{\eta} k_{\eta} = 0 \tag{5}$$

where k_{η} and k_{ξ} are two curvatures of the surface and they were determined by Eq. (2). According to Eq. (2)-Eq. (5), the wrinkles half wavelength λ of a rectangular collector foil subjected to transverse in-plane shear displacement δ, as illustrated in Figure 9, could be predicted by:

$$\lambda^2 = \frac{(kH\pi h)^2}{24\gamma(1-v^2)}\left[\sqrt{\frac{1}{(kH)^4} + \frac{48\gamma(1-v^2)}{(kH\pi h)^2}} - \frac{1}{(kH)^2}\right] \tag{6}$$

The total strain in the η direction is $-\gamma$, while the material strain in this direction is $-v\gamma$. The difference between the two is the “geometric strain”:

$$\varepsilon_G = -\frac{\pi^2 A^2}{4\lambda^2} = -\gamma(1-v) \tag{7}$$

Thus, the amplitude of wrinkles could be solved from Eq. (6) and Eq. (7):

$$A = \frac{2\lambda\sqrt{\gamma(1-v)}}{\pi} + A_0 \tag{8}$$

For better accuracy, a modified value A_0 of 0.03 was employed based on the results of experiments to eliminate deviations resulting from simplified assumptions.

According to the analytical model of wrinkles in the uncoated area, the half wavelength and amplitude of wrinkles were calculated using Eq. (6) and (8) at a front tension of 10N and a tension difference of 5 N, 10 N, 15 N, and 20 N, respectively. The results were compared to the experimental ones, as shown in Figure 11. The predicted results were consistent with the experimental results. For the point where T_d was 20 N, a more significant deviation between analytical and experimental results was observed. With the increase of tension difference to 20 N, the elastic assumption of the foils may no longer correct. Hence the prediction of the wrinkle wave length was over estimated. The model showed a small prediction deviation, in cases where the tension difference was not large enough to make the wrinkles significant. Therefore, the analytical model was applicable within the tension range of concern.

Methods to reduce the wrinkles and corrugations

From the above, a competitive relationship between the wrinkles and corrugations with the increase of the tension difference is revealed. Adjusting the tension parameters to obtain an optimum tension configuration balancing the corrugation and wrinkles in the coated and uncoated areas is thus of significant importance. For that purpose, corrugations and wrinkles were modelled separately, instead of considering the complex boundary and loading conditions. The analytical model developed in previous section reveals the relationship between T_d and the severity of wrinkles. For the corrugations in

the coated area, as depicted in Figure 7(b), the tortuosity ΔC decreases with the increase of the tension difference T_d. As a preliminary study, a simple fitted equation was employed to capture their relationship:

$$\Delta C = 0.23 + 0.304 \exp(-\frac{T_d}{7.62}) \tag{9}$$

With the increase of the tension difference, the tortuosity of the corrugations decreases while the wrinkles become more severe. Therefore, finding an optimal web tension condition with mild corrugations and wrinkles is necessary. In those regards, an evaluation index I was established for trade-offs between these two conflicting objectives:[31]

$$I = \alpha \Delta C + (1 - \alpha) R \tag{10}$$

where α is the weight, the relationship between ΔC and T_d can be obtained by Eq. (9), R is the ratio of amplitude to half wavelength, the relationship between R and T_d can be obtained by Eq. (1), Eq. (6) and Eq. (8). The weight value was taken as 0.2 in this study, considering that the wrinkles in the uncoated area becomes more severe, while the corrugation in the coated area becomes less sensitive with the increase of the tension difference. The value of I was calculated for a range of tension differences T_d using Eq. (10). As illustrated in Figure 12(a), the window for optimized web tensions was determined at a T_d value of 16 to 18 N, where the value of I was minimum.

To validate the previously chosen web tension conditions, experiments on electrode calendering at a tension difference T_d of 17 N were carried out. As shown in Figure 12(b), the corrugations in the coated area were significantly improved, as the tension difference was increased to 17N. Furthermore, little improvement was reached if the tension difference further increased. Meanwhile, the wrinkles in the uncoated area

became more severe with the increase of the tension difference. An abrupt increase in the amplitude to half wavelength ratio of wrinkles was observed with the tension difference reaching 17 N. According to the appearances and height profiles of the calendered electrodes shown in Figure 13, the corrugations were well suppressed without causing excessive wrinkles under the preferred web tension conditions. Therefore, at the point where T_d is 17 N, both the wrinkles and corrugations are limited to an acceptable level, so that a good balance of wrinkles and corrugations is achieved and the best quality calendered electrodes are obtained. The optimal tension condition determined based on the presented method can be effective for the improvement of calendering process.

Conclusions

The effect of web tension is clarified via both experiments and analytical modeling to explore the wrinkles and corrugations on the electrodes during the calendering process. The following conclusive remarks can be drawn:

- The tension difference between the front and back tensions is revealed to be a critical factor affecting the wrinkles and corrugations during electrode calendering. Corrugations in the coated area can be mitigated while the wrinkles in the uncoated area become more evident by increasing the tension difference.
- An analytical prediction model for the wrinkles after calendering is established based on shearing of the rectangular membrane. An evaluation method for the quality of the calendered electrode is developed to balance the effects of wrinkles and corrugations.

- An optimal web tension parameter to improve the quality of calendered electrodes is achieved at T_d of 17 N and the predicted results are consistent with the experimental results.
- The method and results presented in this paper is expected for the optimization in the calendering process for lithium-ion battery electrodes to minimize both the wrinkles and corrugations.

Disclosure statement

The authors report there are no competing interests to declare.

Funding

This work was supported by the [National Natural Science Foundation of China] under Grant (52225504 and 52275353); and [Research Projects of National Key Laboratory for Precision Hot Processing of Metals] under Grant (No. JCKYS2022603C009).

References

[1] Li, J.; Fleetwood, J.; Hawley, W. B.; Kays, W. From Materials to Cell: State-of-the-Art and Prospective Technologies for Lithium-Ion Battery Electrode Processing. *Chem. Rev.* 2022, *122*(1), 903-956. DOI: 10.1021/acs.chemrev.1c00565.

[2] Zeng, F.; Zhang, Y.; Shao, Z. Synthesis and Electrochemical Performance of Mo-doped $LiNi_{0.5}Mn_{1.5}O_4$ Cathode Material. *Mater. Manuf. Process.* 2022, *38*(2), 197-205. DOI: 10.1080/10426914.2022.2075885.

[3] Kumawat, S.; Singh, D.; Saini, A. Recycling of Spent Lithium-Iron Phosphate Batteries: Toward Closing the Loop. *Mater. Manuf. Process.* 2022, *38*(2), 135-150. DOI: 10.1080/10426914.2022.2136387.

[4] Kappes, B. B.; Ciobanu, C. V. Materials Screening Through GPU Accelerated Topological Mapping. *Mater. Manuf. Process.* 2015, *30*(4), 529–537. DOI: 10.1080/10426914.2014.984215.

[5] Yang, K.; Xie, X.; Du, X.; Zuo, Y.; Zhang, Y. Research on Micromechanical Behav

ior of Current Collector of Lithium-Ion Batteries Battery Cathode during the Calen dering Process. *Processes.* 2023, *11*(6), 1800. DOI: 10.3390/pr11061800.

[6] Örüm Aydin, A.; Zajonz, F.; Günther, T.; Dermenci, K. B.; Berecibar, M.; Urrutia, L. Lithium-Ion Battery Manufacturing: Industrial View on Processing Challenges, Possible Solutions and Recent Advances. *Batteries.* 2023, *9*(11), 555. DOI: 10.339 0/batteries9110555.

[7] Sim, R.; Lee, S.; Li, W. D.; Manthiram, A. Influence of Calendering on the Electro chemical Performance of $LiNi_{0.9}Mn_{0.05}Al_{0.05}O_2$ Cathodes in Lithium-Ion Cells. *ACS Appl. Mater. Interfaces.* 2021, *13*(36), 42898-42908. DOI: 10.1021/acsami.1c125 43.

[8] Kim, J.; Park, K.; Kim, M.; Lee, H.; Choi, J.; Park, H. B.; Kim, H.; Jang, J.; Kim, Y. H.; Song, T.; Paik, U. 10 mAh cm^{-2} Cathode by Roll-to-Roll Process for Low Co st and High Energy Density Li-Ion Batteries. *Adv. Energy Mater.* 2024, *14*, 230345 5. DOI: 10.1002/aenm.202303455.

[9] Zhu, J.; Li, W.; Wierzbicki, T.; Xia, Y.; Harding, J. Deformation and Failure of Lith ium-Ion Batteries Treated as a Discrete Layered Structure. *Int. J. Plast.* 2019, *121*, 293-311. DOI: 10.1016/j.ijplas.2019.06.011.

[10] Kwade, A.; Haselrieder, W.; Leithoff, R.; Modlinger, A.; Dietrich, F.; Droeder, K. Current Status and Challenges for Automotive Battery Production Technologies. *N at. Energy.* 2018, *3*, 290-300. DOI: 10.1038/s41560-018-0130-3.

[11] Wang, D.; Wang, G.; Xu, C.; Liu, H. Mechanics and Deformation Behavior of Lith ium-Ion Battery Electrode during Calendering Process. *J. Energy Storage.* 2024, *8 7*, 111521. DOI: 10.1016/j.est.2024.111521.

[12] Günther, T.; Schreiner, D.; Metkar, A.; Meyer, C.; Kwade, A.; Reinhart, G. Classifi cation of Calendering-Induced Electrode Defects and Their Influence on Subseque nt Processes of Lithium-Ion Battery Production. *Energy Technol.* 2020, *8*, 190002 6. DOI: 10.1002/ente.201900026.

[13] Mayer, D.; Wurba, A.-K.; Bold, B.; Bernecker, J.; Smith, A.; Fleischer, J. Investigat ion of the Mechanical Behavior of Electrodes after Calendering and Its Influence o n Singulation and Cell Performance. *Processes.* 2021, *9*(11), 2009. DOI: 10.3390/ pr9112009.

[14] Mayer, D.; Fleischer, J. Concept for Modelling the Influence of Electrode Corrugat ion after Calendering on Stacking Accuracy in Battery Cell Production. *Procedia C*

IRP. 2021，*104*, 744-749. DOI: 10.1016/j.procir.2021.11.125.

[15] Mayr, A.; Schreiner, D.; Stumper, B.; Daub, R. In-Line Sensor-Based Process Control of the Calendering Process for Lithium-Ion Batteries. *Procedia CIRP.* 2022，*107*, 295-301. DOI: 10.1016/j.procir.2022.04.048.

[16] Abdollahifar, M.; Cavers, H.; Scheffler, S.; Diener, A.; Lippke, M.; Kwade, A. Insights into Influencing Electrode Calendering on the Battery Performance. *Adv. Energy Mater.* 2023，*13*, 2300973. DOI: 10.1002/aenm.202300973.

[17] Schreiner, D.; Zünd, T.; Günter, F. J.; Kraft, L.; Stumper, B.; Linsenmann, F.; Schüßler, M.; Wilhelm, R.; Jossen, A.; Reinhart, G.; et al. Comparative Evaluation of LMR-NCM and NCA Cathode Active Materials in Multilayer Lithium-Ion Pouch Cells: Part I. Production, Electrode Characterization, and Formation. *J. Electrochem. Soc.* 2021，*168*, 030507. DOI: 10.1149/1945-7111/abe50c.

[18] Zhang, C.; Xu, J.; Cao, L.; Wu, Z. N.; Santhanagopalan, S. Constitutive Behavior and Progressive Mechanical Failure of Electrodes in Lithium-Ion Batteries. *J. Power Sources.* 2017，*357*, 126-137. DOI: 10.1016/j.jpowsour.2017.04.103.

[19] Zhang, C.; Santhanagopalan, S.; Sprague, M. A.; Pesaran, A. A. Coupled Mechanical-Electrical-Thermal Modeling for Short-Circuit Prediction in a Lithium-Ion Cell under Mechanical Abuse. *J. Power Sources.* 2015，*290*, 102-113. DOI: 10.1016/j.jpowsour.2015.04.162.

[20] Gupta, P.; Üçel, İ. B.; Gudmundson, P.; Olsson, E. Characterization of the Constitutive Behavior of a Cathode Active Layer in Lithium-Ion Batteries Using a Bending Test Method. *Exp. Mech.* 2020，*60*, 847-860. DOI: 10.1007/s11340-020-00613-5.

[21] Meyer, C.; Bockholt, H.; Haselrieder, W.; Kwade, A. Characterization of the Calendering Process for Compaction of Electrodes for Lithium-Ion Batteries. *J. Mater. Process. Technol.* 2017，*249*, 172-178. DOI: 10.1016/j.jmatprotec.2017.05.031.

[22] Meyer, C.; Kosfeld, M.; Haselrieder, W.; Kwade, A. Process Modeling of the Electrode Calendering of Lithium-Ion Batteries Regarding Variation of Cathode Active Materials and Mass Loadings. *J. Energy Storage.* 2018，*18*, 371-379. DOI: 10.1016/j.est.2018.05.018.

[23] Zhu, J.; Li, W.; Xia, Y.; Sahraei, E. Testing and Modeling the Mechanical Properties of the Granular Materials of Graphite Anode. *J. Electrochem. Soc.* 2018，*165*, A1160-A1168. DOI: 10.1149/2.0141807jes.

[24] Sahraei, E.; Bosco, E.; Dixon, B.; Lai, B. Microscale failure mechanisms leading t o internal short circuit in Li-ion batteries under complex loading scenarios. *J. Powe r Sources.* 2016, *319*, 56-65. DOI: 10.1016/j.jpowsour.2016.04.005.

[25] Sahraei, E.; Hill, R.; Wierzbicki, T. Calibration and finite element simulation of po uch lithium-ion batteries for mechanical integrity. *J. Power Sources.* 2012, *201*, 30 7-321. DOI: 10.1016/j.jpowsour.2011.10.094.

[26] Lundkvist, A.; Larsson, P.-L.; Olsson, E. A Discrete Element Analysis of the Mech anical Behaviour of a Lithium-Ion Battery Electrode Active Layer. *Powder Technol.* 2023, *425*, 118574. DOI: 10.1016/j.powtec.2023.118574.

[27] Diener, A.; Ivanov, S.; Haselrieder, W.; Kwade, A. Evaluation of Deformation Beha vior and Fast Elastic Recovery of Lithium-Ion Battery Cathodes via Direct Roll-Ga p Detection During Calendering. *Energy Technol.* 2022, *10,* 2101033. DOI: 10.100 2/ente.202101033.

[28] Mayer, D.; Schwab, B.; Fleischer, J. Influence of Electrode Corrugation after Calen dering on the Geometry of Single Electrode Sheets in Battery Cell Production. *Ene rgy Technol.* 2023, *11*, 2200870. DOI: 10.1002/ente.202200870.

[29] Djavanroodi, F.; Abbasnejad, D. S.; Nezami, E. H. Deep Drawing of Aluminum All oys Using a Novel Hydroforming Tooling. *Mater. Manuf. Process.* 2011, *26*(5), 79 6-801. DOI: 10.1080/10426911003720722.

[30] Wang, C. G.; Tan, H. F.; Du, X. W.; Wan, Z. M. Wrinkling Prediction of Rectangul ar Shell-Membrane under Transverse In-Plane Displacement. *Int. J. Solids Struct.* 2 007, *44*, 6507-6516. DOI: 10.1016/j.ijsolstr.2007.02.036.

[31] Flegiel, F.; Sharma, S.; Rangaiah, G. P. Development and Multiobjective Optimizat ion of Improved Cumene Production Processes. *Mater. Manuf. Process.* 2015, *30* (4), 444–457. DOI: 10.1080/10426914.2014.967355.

Figures

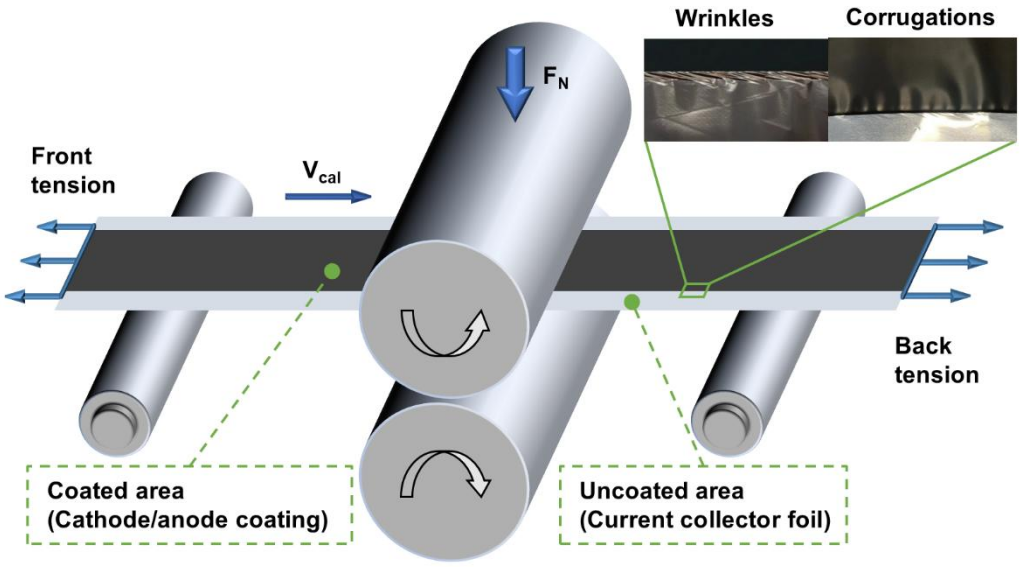

Figure 1. Schematic of the calendering process of lithium-ion battery electrodes.

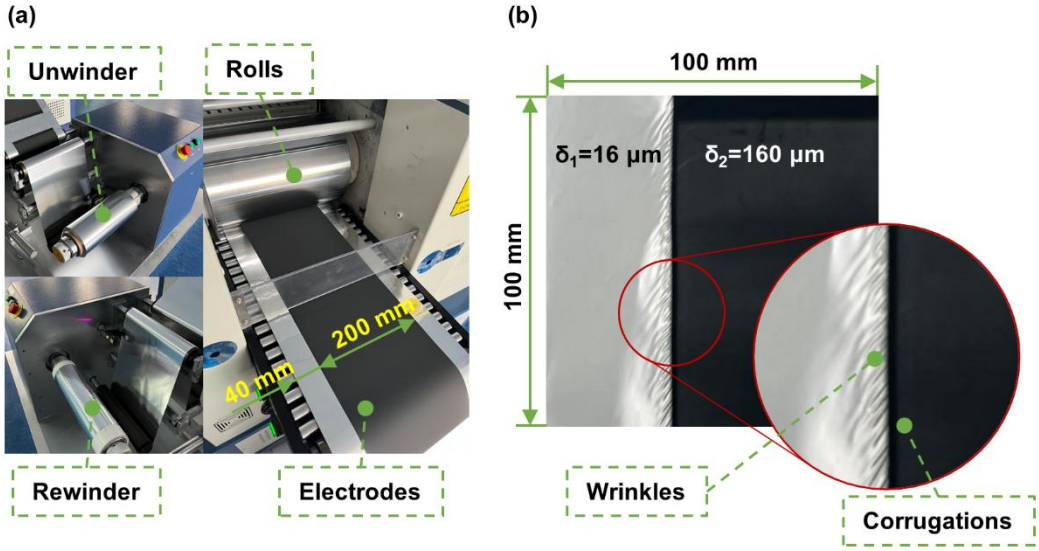

Figure 2. Experimental procedures: (a) electrodes calendering systems; (b) images of electrodes after calendering.

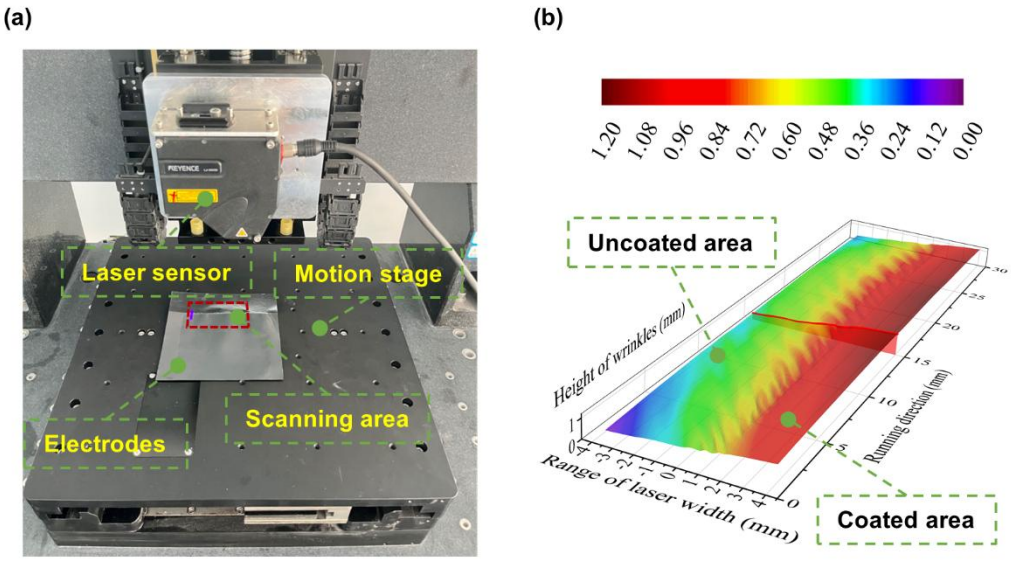

Figure 3. (a) Calendered electrodes and measurement devices; (b) Three-dimensional topography of the calendered electrodes.

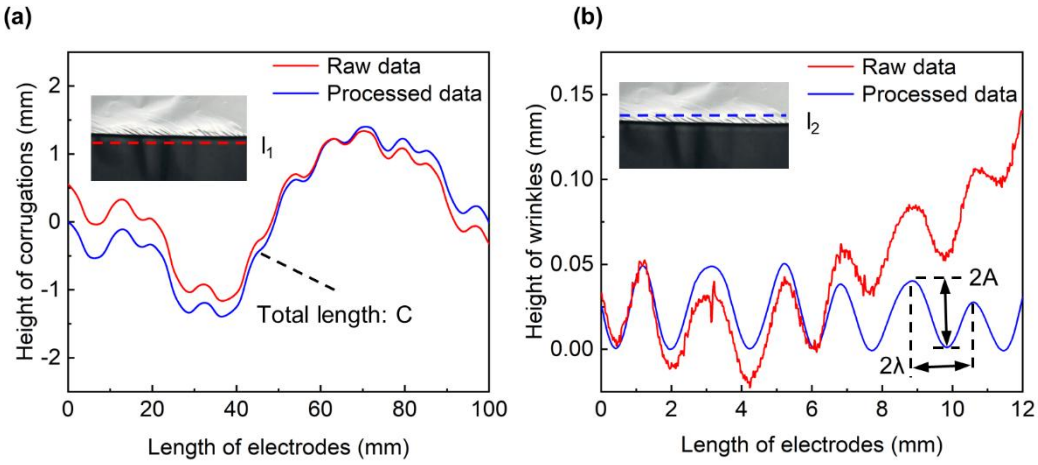

Figure 4. Evaluation of calendered electrodes, (a) corrugations in the coated area, and (b) wrinkles in the uncoated area of electrodes.

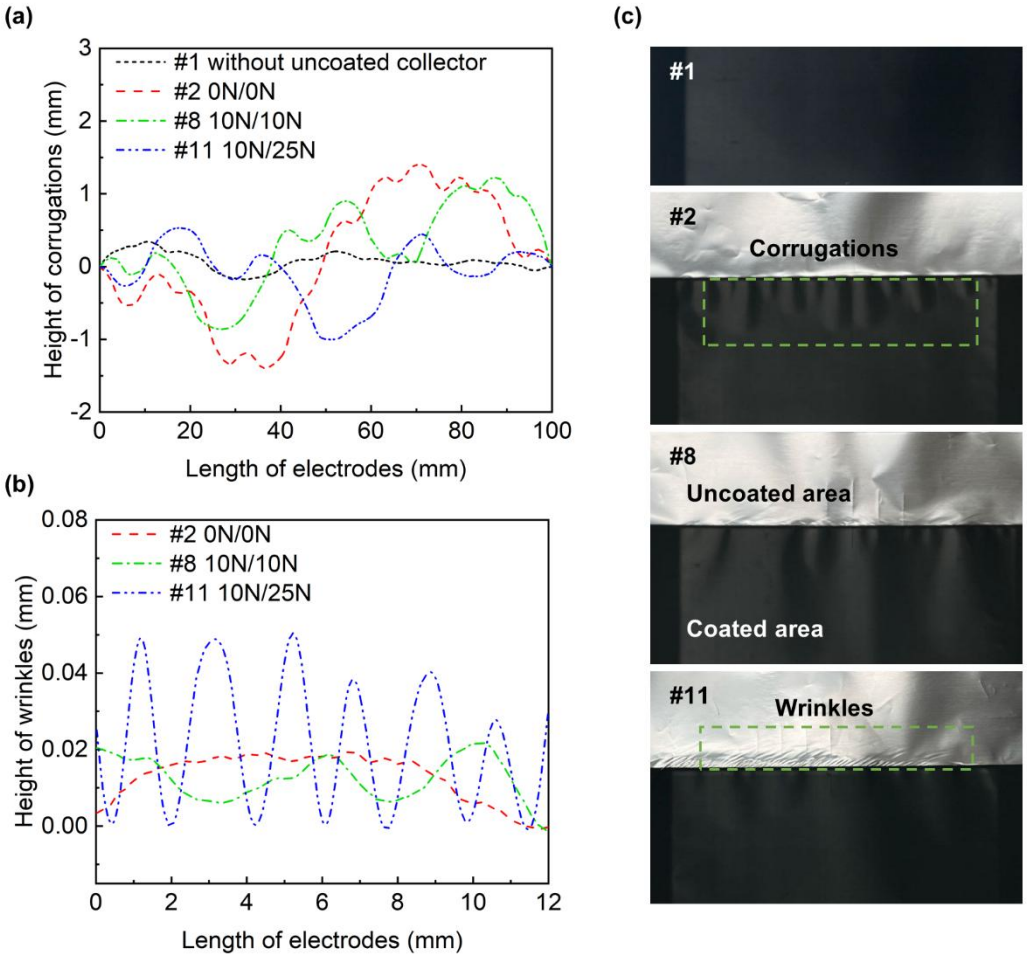

Figure 5. Height profiles of the electrodes under different conditions: (a) corrugations in coated area; (b) wrinkles in uncoated area; (c) the photographs of wrinkles and corrugations after calendering.

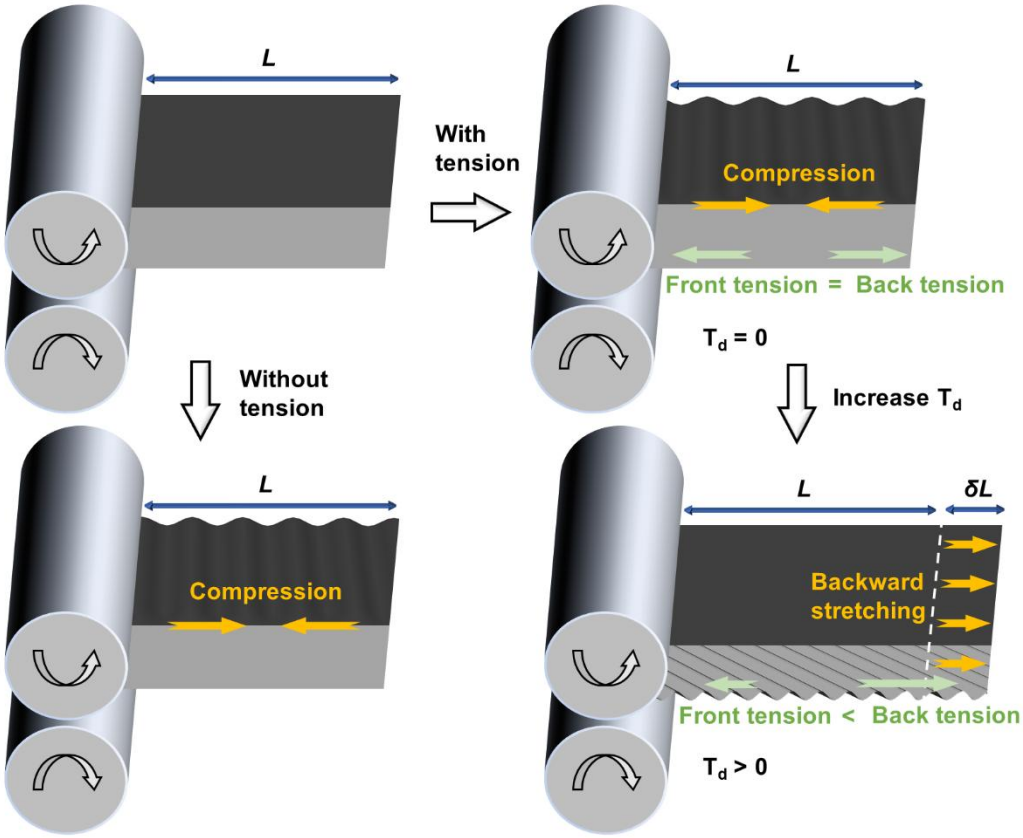

Figure 6. Schematic of the wrinkling and corrugating behavior of the electrodes during calendering.

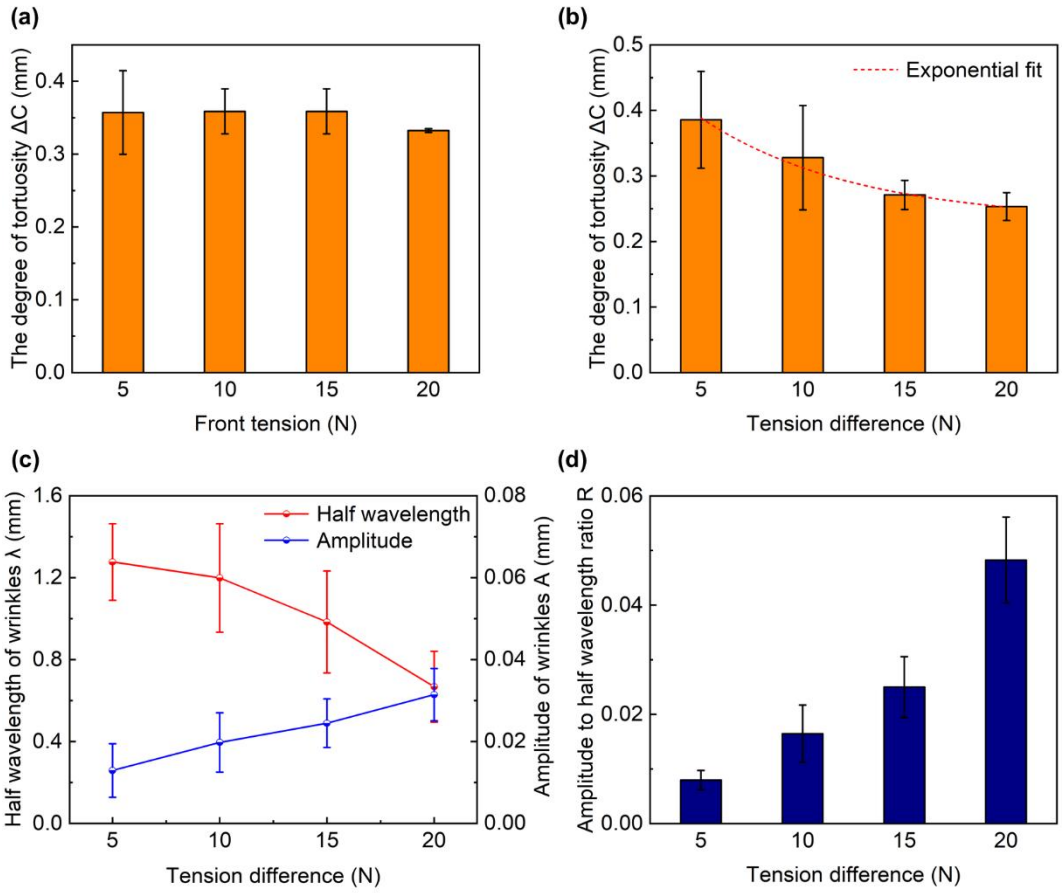

Figure 7. Effect of the web tension on corrugations, (a) front tension equals back tension; (b) front tension was 10 N, and the tension difference increases; and on wrinkles: (c) the half wavelength and amplitude, and (d) the ratio of amplitude to half wavelength, at a front tension of 10 N.

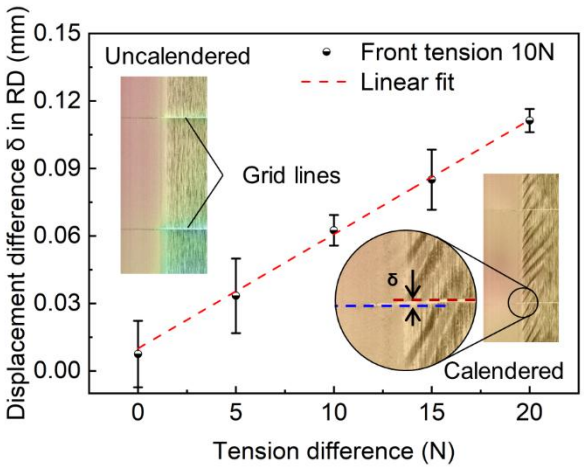

Figure 8. Relationship between shear displacement and tension difference.

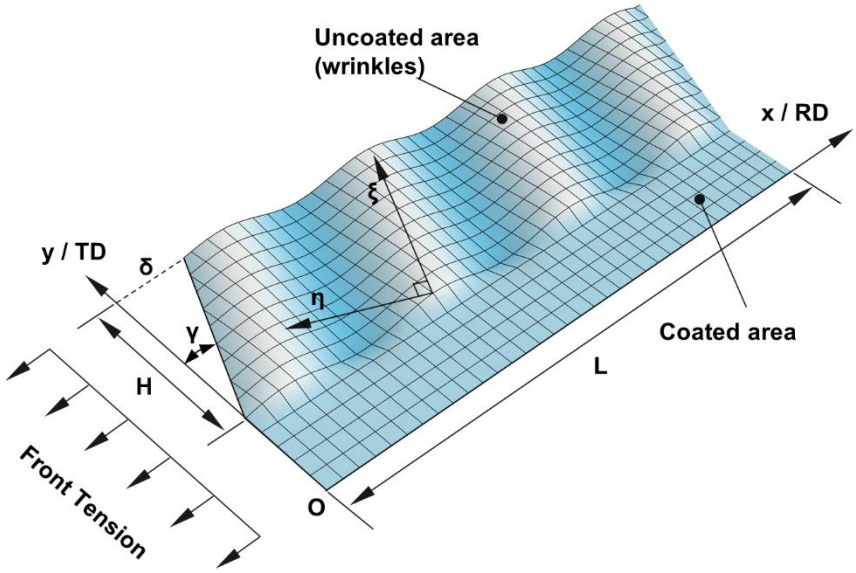

Figure 9. Analytical model of shear wrinkling in the uncoated area of electrodes.

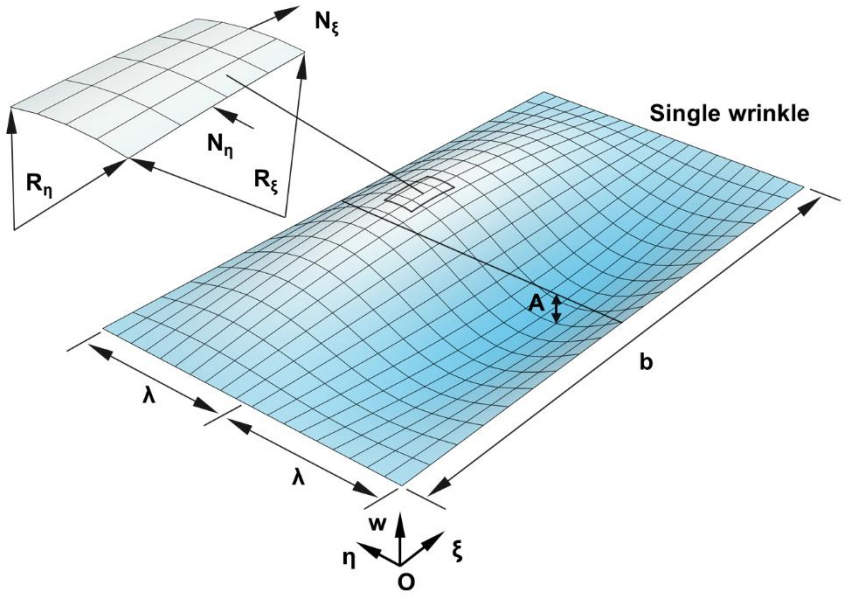

Figure 10. Schematic of a single wrinkle and force equilibrium relationship.

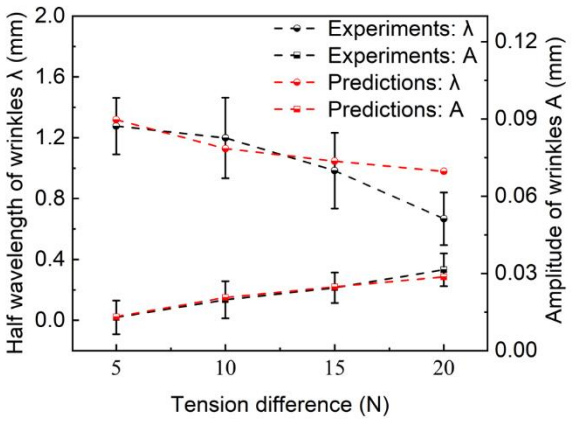

Figure 11. Prediction of wrinkles: experimental and predicted results under different tension differences.

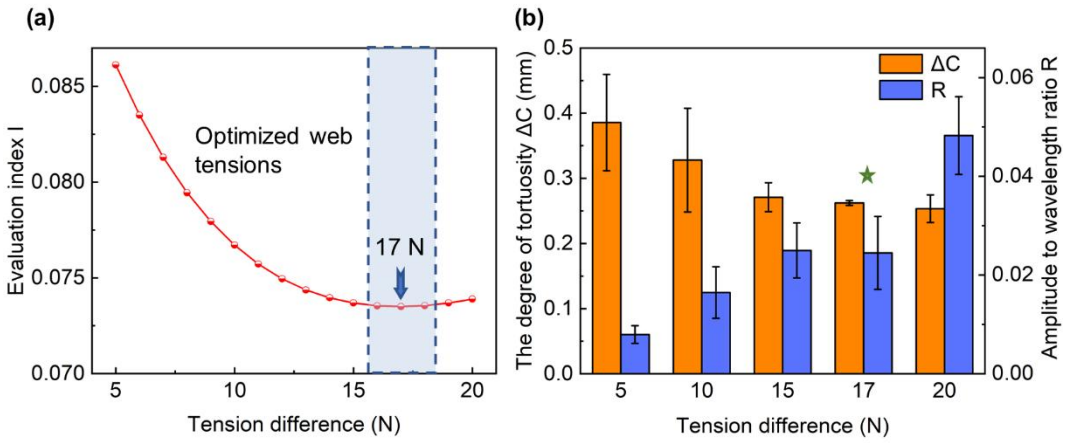

Figure 12. (a) Determination of the optimal web tension conditions; (b) Validation of the selected web tension conditions: the tortuosity ΔC and amplitude to half wavelength ratio R of calendered electrodes under different tension differences.

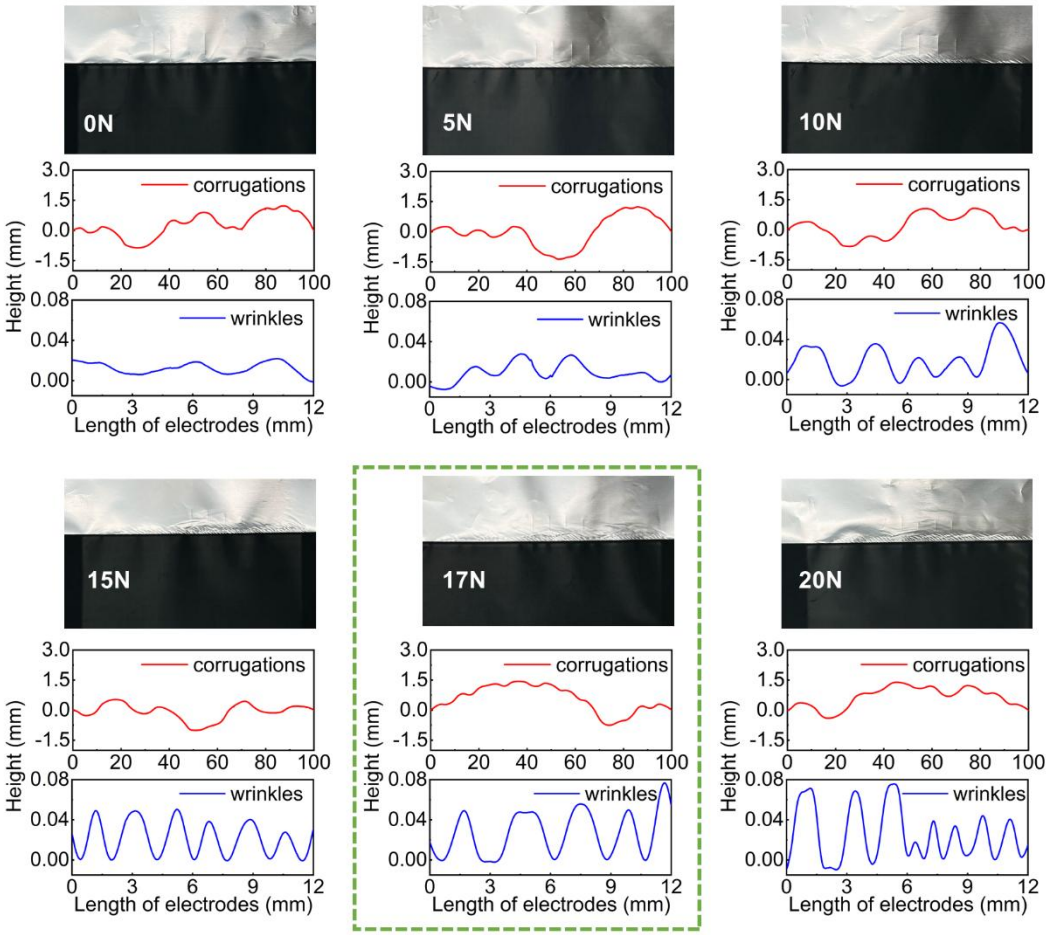

Figure 13. Photographs recording the appearance of calendered electrodes and the corresponding wrinkles and corrugations height profiles under different web tension conditions.

Tables

Table 1. Overview of the design of experiments.

No.	Front Tension (N)	Back Tension (N)	Collector Width (mm)
1	10	25	0
2	0	0	40
3	5	5	40
4	5	10	40
5	5	15	40
6	5	20	40
7	5	25	40
8	10	10	40
9	10	15	40
10	10	20	40
11	10	25	40
12	10	30	40
13	15	15	40
14	15	20	40
15	15	25	40
16	15	30	40
17	15	35	40
18	20	20	40
19	20	25	40
20	20	30	40
21	20	35	40
22	20	40	40